Expanded View Figures

Figure EV1. Density of Mmi1 binding sites within mRNAs and lncRNAs, and computational approach developed to predict Mmi1 RNA targets.

A Density of Mmi1 binding motif (UNAAAC) among all the annotated mRNAs and lncRNAs versus the mRNAs and lncRNAs enriched at least twofold in Mmi1 RNA-IP Seq.

B Diagram of the genomewide computational approach used to predict Mmi1 targets. In step 1, a hypothetical open reading frame that has eight UNAAAC motifs in its sequence is shown as an example. The double-headed arrows indicate all possible windows containing from two to eight motifs. The thick double-headed arrows correspond to the windows yielding the minimal window size (MWS) from two to eight motifs. In step 2, each box plot represents the MWS^x calculated for all of the validated targets. The boxplots were produced using the "boxplot" function in R with default parameters: the boxes represent the median and the upper and lower quartiles (25% and 75%); and the whiskers attempt to capture the extreme values, but extend to at most 1.5 times the interquartile range from the box, in which case any outliers beyond this range appear as crosses. The numbers in red represent the cutoff window size (CWS) for two to eight motifs. See the Materials and Methods for more details.

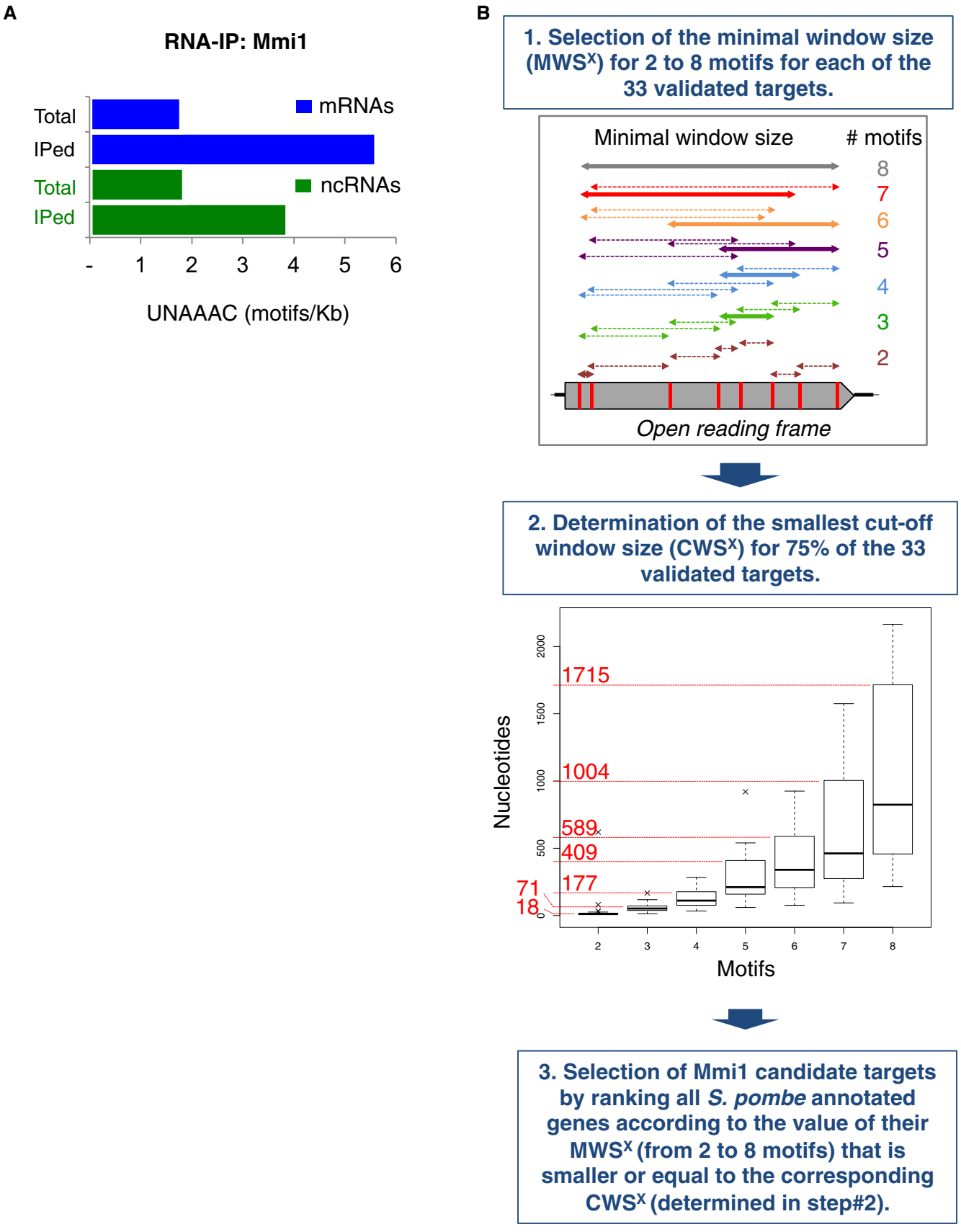

Figure EV1.

Figure EV2. Characterization of Mmi1 YTH domain point mutants R351E and R381E.

A Sequence alignment of YTH domains from the yeast *Schizosaccharomyces pombe* (*Sp*), the yeast *Zygosaccharomyces rouxii* (*Zr*), and *Homo sapiens* (*Hs*).
B Ribbon diagram of Mmi1 YTH domain structure in the same orientation as in Fig 2C.
C RNA-IP showing that the *in vivo* binding of Mmi1 to three of its known targets (*ssm4*, *rec8*, and *spo5* mRNAs) is strongly reduced for R351E and R381E Mmi1 mutants.
D Gel filtration showing similar elution behavior for WT, R351E, and R381E Mmi1 YTH domains.
E RNA pull-down showing *in vitro* that mutations R351E and R381E impair Mmi1 binding to a RNA containing the UUAAAC motif.
F Relative enrichments of Mmi1 protein recovered after RNA pull-downs done in (E). The quantification was estimated from three independent experiments. See the Materials and Methods for more details.
G Fluorescence microscopy images showing the cellular localization of Mmi1-R351E, Mmi1-R381E and Mmi1 wild-type (WT) proteins. Nuclear DNA was stained with DAPI (blue). Scale bar, 10 μm.

Data information: Average fold enrichment is shown with error bars that indicate mean average deviations ($n = 3$) for (C, F).
Source data are available online for this figure.

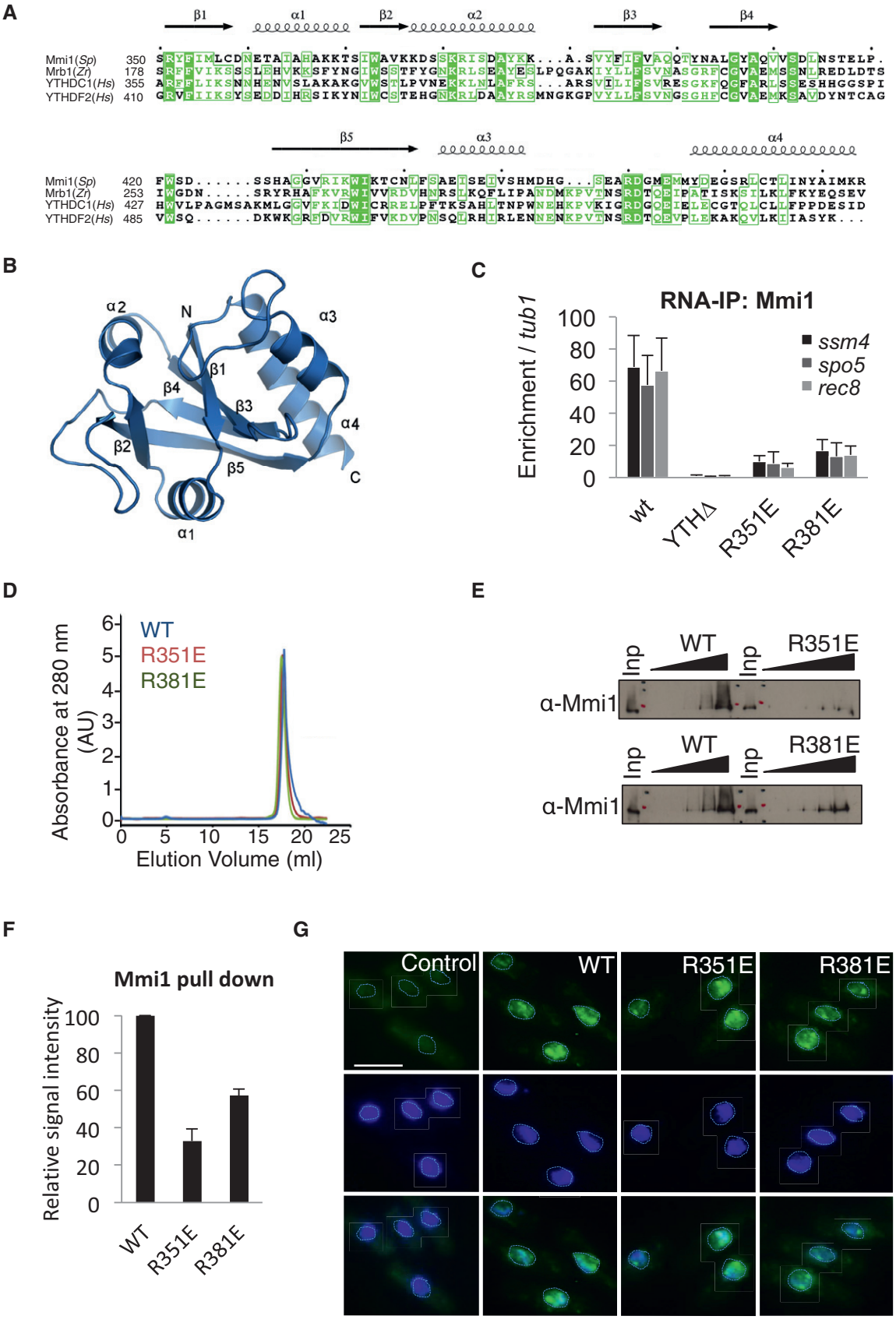

Figure EV2.

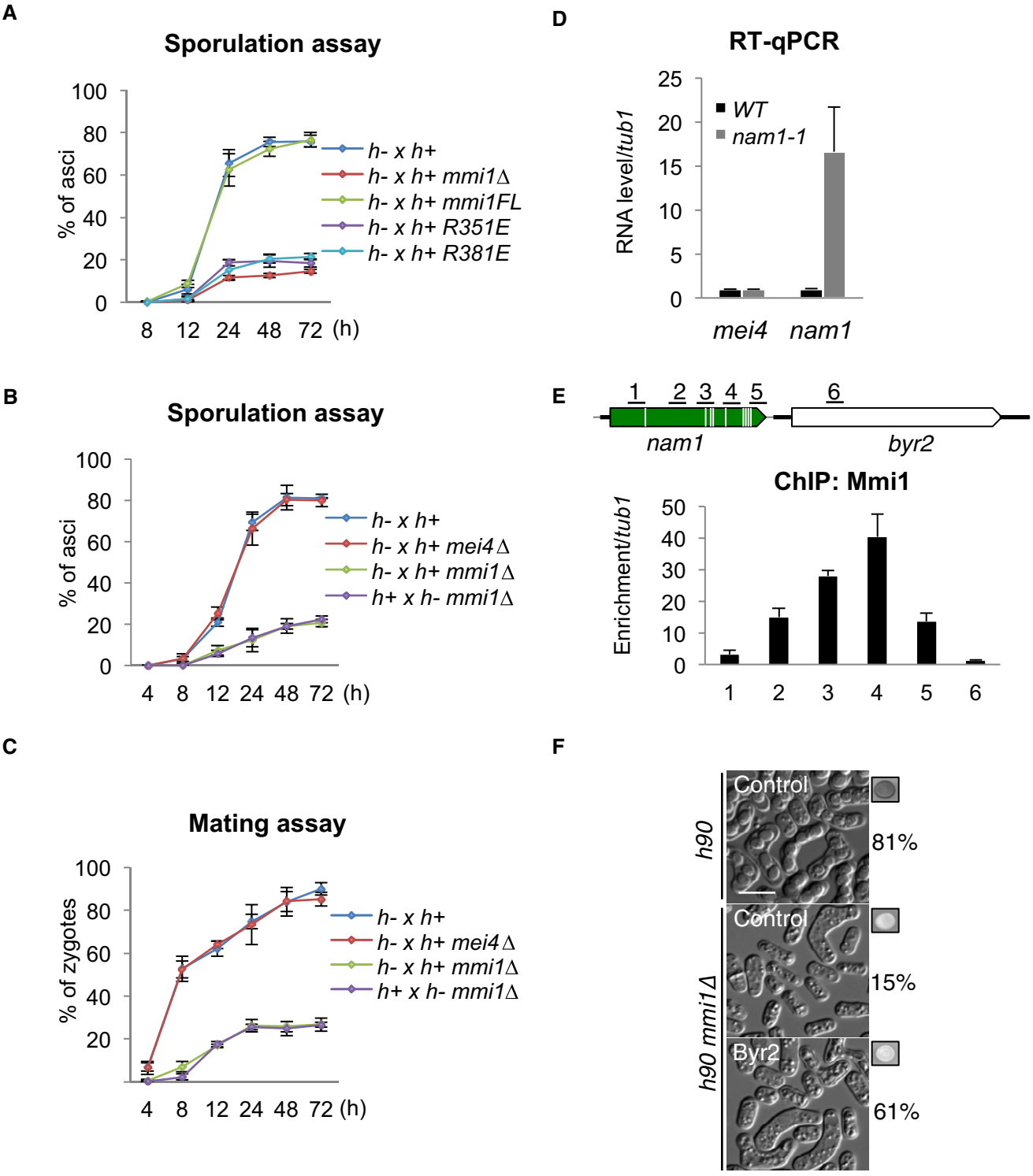

Figure EV3.

Figure EV3. Mmi1-dependent entry into sexual differentiation (related to Fig 2).

A Sporulation assay showing the percentage of asci forming over time in *WT*, *mmi1*Δ, *mmi1-R351E*, and *mmi1-R381E* cells.
B, C Graphs showing the percentage of asci (B) and zygotes (C) forming over time in *WT*, *mei4*Δ, and *mmi1*Δ *mei4*Δ cells.
D RT–qPCR showing the level of *nam1* lncRNA and *mei4* mRNA in *WT* and *nam1-1* cells.
E ChIP monitoring Mmi1 localization over *nam1-byr2* locus in *WT* cells. Upper part of the panel highlights genomic regions (black lines).
F Microscopy images showing the state of sexual differentiation of *WT* and *mmi1*Δ cells expressing or not expressing Byr2 from a plasmid, after 24 h of growth on SPAS. The percentage of cells that underwent differentiation and iodine vapor assays conducted on the corresponding patch are shown at the right side of each picture. Scale bar, 10 μm.

Data information: Average fold enrichment is shown with error bars that indicate mean average deviations (n = 3) for (A–E).

Figure EV4. Mmi1 control of *byr2* gene expression (related to Fig 3).

A RT–qPCR showing the accumulation of *nam1* read-through transcripts in *nam1-1* cells. Black arrow, primer used for the strand-specific reverse transcription (RT); black line, location of the region amplified by PCR.
B ChIPs showing the occupancy of the whole population of RNAPII over *nam1-byr2* locus, in *WT* and *nam1-1* cells. Black lines above the scheme, genomic regions investigated.
C ChIPs showing the occupancy of the elongating RNAPII (RNAPII-S2P) over *nam1-byr2* locus, in *WT* and *mmi1*Δ cells. The same genomic regions as in (B) were investigated.
D ChIPs showing the occupancy of the initiating RNAPII (RNAPII-S5P) over *nam1-byr2* locus, in *WT* and *nam1-1* cells. The same genomic regions as in (B) were investigated.
E Microscopy images showing the sexual differentiation status in *WT*, *mmi1*Δ, and *mmi1*Δ *nam1-Ttef* cells, after 24 h of growth on SPAS. The percentage of cells that underwent differentiation and iodine vapor assays conducted on the corresponding patch are shown at the right side of each picture. Scale bar, 10 μm.
F Northern blot showing the level of *byr2* mRNA before (0 h) and after (0.5 h) induction of sexual differentiation in *WT*, *nam1-1*, *nam1-Ttef*, and in *nam1-1-Ttef*. Note that the white separation indicates that lanes on the left and the right come from the same gel but that the images were cropped to place them next to each other.
G Microscopy images showing *WT* cells transformed with an empty plasmid or a pREP plasmid expressing *nam1-L* or *nam1-1L* lncRNA, after having induced sexual differentiation by growth on SPAS for 24 h. Scale bar, 10 μm.
H RT–qPCR showing the level of *nam1-L* and *nam1-1-L* lncRNA expressed from the pREP plasmid.
I Microscopy images showing *WT* (*h90*) and *rrp6*Δ cells, after having induced sexual differentiation by growth on SPAS for 24 h. Scale bar, 10 μm.
J Mating assay showing the percentage of zygotes forming over a 72-h period, from cells induced to undergo sexual differentiation by growth on SPAS.
K ChIP showing the enrichment of Rrp6 over *nam1-byr2* locus.
L ChIP monitoring the enrichment of H3K9me2 over *nam1-byr2* locus and *mei4* gene in *WT* and *mmi1*Δ cells.

Data information: Average fold enrichment is shown with error bars that indicate mean average deviations (n = 3) for (A–D, H, J–L).
Source data are available online for this figure.

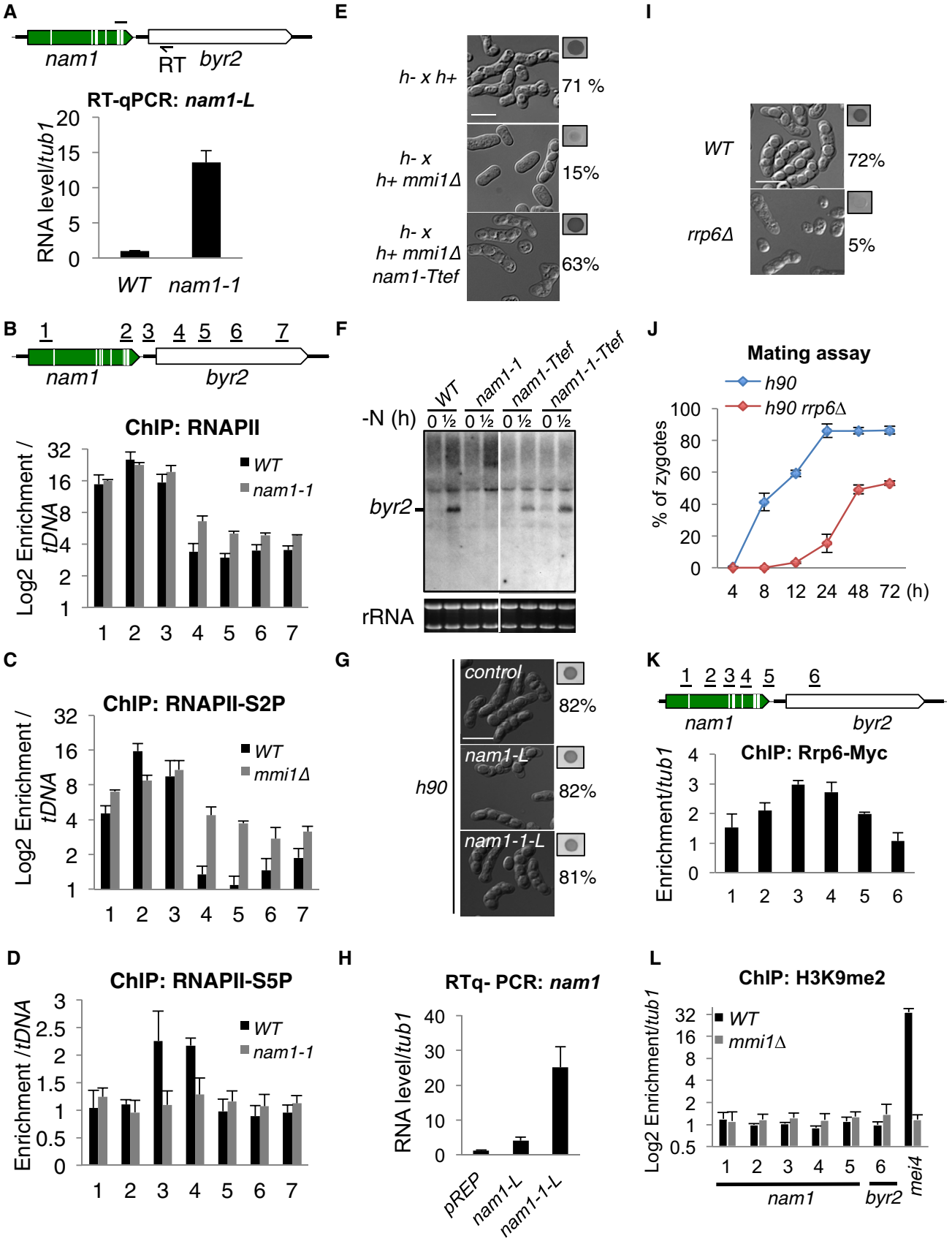
A
nam1
RT
byr2
RT-qPCR: nam1-L
RNA level/tub1
WT
nam1-1
B
nam1
byr2
ChIP: RNAPII
Log2 Enrichment / tDNA
WT
nam1-1
C
ChIP: RNAPII-S2P
WT
mmi1Δ
D
ChIP: RNAPII-S5P
Enrichment /tDNA
E
h- x h+
71 %
h- x h+ mmi1Δ
15%
h- x h+ mmi1Δ nam1-Ttef
63%
F
WT
nam1-1
nam1-Ttef
nam1-1-Ttef
-N (h)
0 ½
byr2
rRNA
G
control
82%
h90
nam1-L
82%
nam1-1-L
81%
H
RTq- PCR: nam1
RNA level/tub1
pREP
nam1-L
nam1-1-L
I
WT
72%
rrp6Δ
5%
J
Mating assay
h90
h90 rrp6Δ
% of zygotes
4 8 12 24 48 72 (h)
K
nam1
byr2
ChIP: Rrp6-Myc
Enrichment/tub1
L
ChIP: H3K9me2
Log2 Enrichment/tub1
WT
mmi1Δ
nam1
byr2
mei4

Figure EV4.

Figure EV5. Mmi1-directed heterochromatin gene silencing (related to Fig 4).

A RNA-IP showing that *in vivo*, the binding of Mmi1 to *nam5/6/7* lncRNAs is strongly reduced by Mmi1 mutations R351E and R381E expressed from a plasmid.
B RNA-IP showing that Mmi1 binds to *nam5/6/7* lncRNAs but not to *dg* lncRNAs.
C RT–qPCR showing the synergy of accumulation of *nam5/6/7* lncRNAs in *mmi1-ts3 clr4*Δ double mutant cells at restrictive temperature (36°C).
D RT–qPCR showing no additional accumulation of *dg* lncRNAs in *mmi1-ts3 dcr1*Δ double mutant cells at restrictive temperature (36°C).
E ChIP showing a reduction of the level of H3K9me2 at the *nam5/6/7* and *dg* pericentromeric regions but not at *mei4* gene, in cells overexpressing Mmi1 (*pnmt1-mmi1*) compared to *WT* cells. *P*-value was calculated from four independent experiments using a two-tailed Student's *t*-test.
F RT–PCRs monitoring the accumulation of *nam7-L* in *WT*, *clr4*Δ, and *mmi1*Δ and *mmi1*Δ *clr4*Δ cells. In the upper part of the panel, the black arrows indicate the location of the primers used for reverse transcription (RT), and the black lines indicate the expected PCR products.
G ChIPs showing the occupancy of the elongating RNAPII (RNAPII-S2P) over *dh* repeats in *WT*, *mmi1*Δ, *clr4*Δ, and *mmi1*Δ *clr4*Δ cells. Black lines above the scheme, genomic regions investigated.
H RNA-IP showing that Cid14 is not required for the association of Rrp6-Myc13 to *nam5/6/7* lncRNAs.
I RT–PCRs monitoring the accumulation of *nam7-L* in *rrp6*Δ, *dcr1*Δ, and *rrp6*Δ and *dcr1*Δ cells. RT–PCRs were conducted using the same conditions as in (F).

Data information: Average fold enrichment is shown with error bars that indicate mean average deviations ($n = 3$) for (B–D, G and H) and ($n = 4$) for (E).
Source data are available online for this figure.

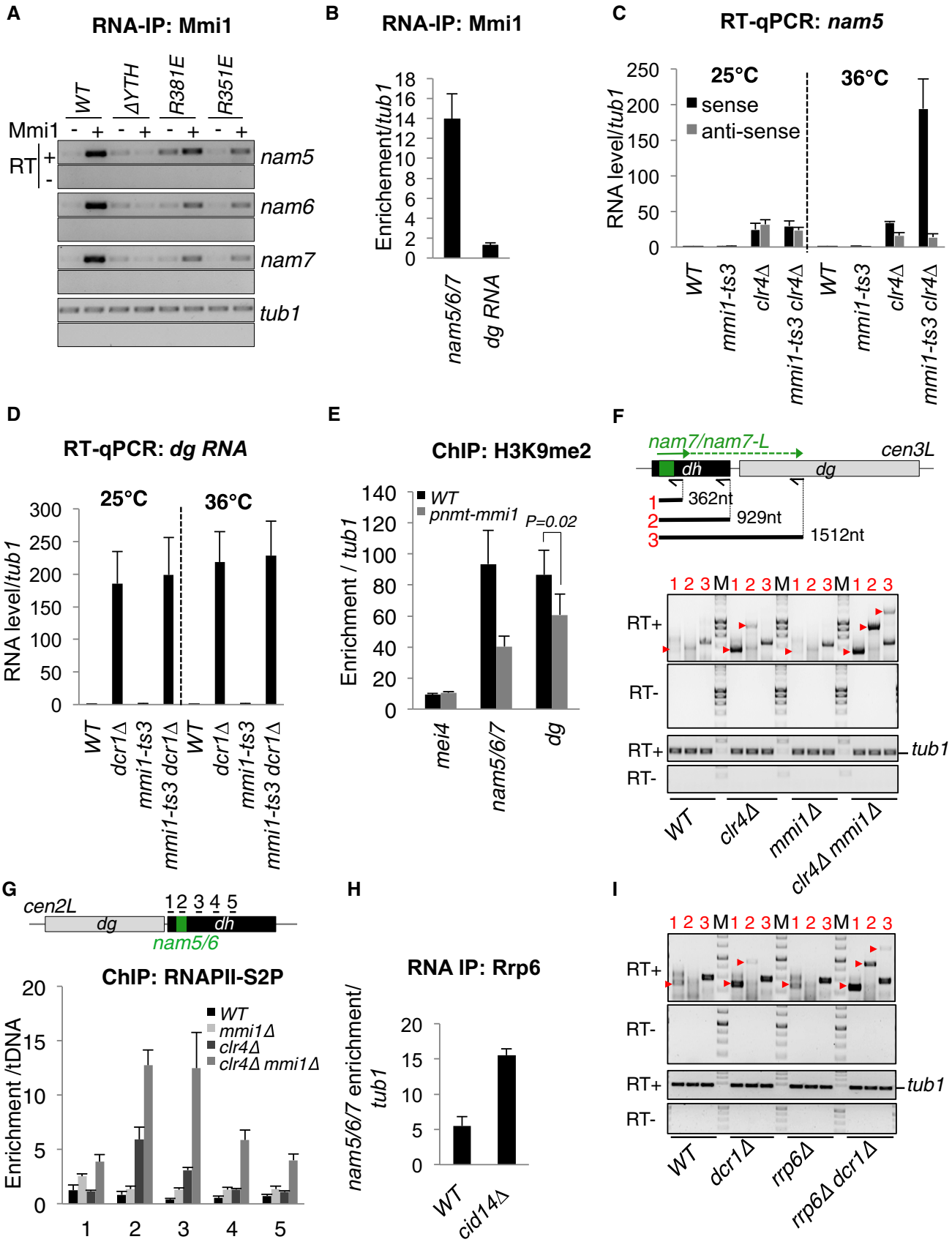

Figure EV5.